

# Capacity Value of Large Tidal Barrages

J. Radtke, C.J. Dent, *Member, IEEE* and S.J. Couch

**Abstract**—This paper presents the first detailed capacity value calculation for tidal barrage generation, based on modelling of operational modes for the proposed 8 GW Severn Barrage scheme in Great Britain. The key finding is that the Effective Load Carrying Capability is very low as a percentage of installed capacity (less than 10% for the example presented here). This is because of the high probability of having zero available output at time of peak demand, if peak demand occurs on the wrong part of the tidal cycle; this result may be explained transparently using a simple two-state model of the barrage. The prospects for building a probabilistic model of tidal barrage availability are also discussed.

**Index Terms**—Tidal power generation, Power system reliability

## I. INTRODUCTION

THE availability of renewable generation capacity is primarily determined by natural resource availability; as a result, renewable technologies are often referred to as having variable output (wind generation availability is variable and unpredictable, whereas tidal output is variable and predictable.) Their ability to support demand is thus qualitatively different from that of conventional generating plant, which is able to generate at maximum output provided it is mechanically available and has an adequate fuel supply.

Tidal barrage power plants are one example of renewable generation technology, and are attractive in Great Britain because of the high available tidal range; they generate power by exploiting the difference in sea level between high and low tide (see Chapter 6 of [1]). Britain's tidal potential is dominated by the proposed Severn Barrage scheme, which if built could have an installed capacity of around 8 GW [2].

The concept of capacity value is important in quantifying the contribution of renewables to support demand, and in comparing this to the contribution of conventional plant. The most common definition of capacity value (referred to as Effective Load Carrying Capability, or ELCC) is the additional demand which the generation unit (or ensemble thereof) can support without increasing the chosen measure of system risk. To date, most of the work on capacity value of renewables has concentrated on wind generation, e.g. [3]. There has been one previous study on the capacity value of tidal current generation [4]; we believe that this paper is the first detailed study of the

capacity value of tidal barrage generation (an earlier result based on less detailed modelling has been published in [5]).

The next part of the paper provides background on capacity value calculations (Section II) and tidal modelling (Section III) to motivate the new work. Section IV then presents a capacity value study for the Severn Barrage, based on modelling of operational modes for the scheme, and Section V demonstrates how a simple two state model of the barrage's availability can explain transparently the Severn Barrage results (the capacity value is found to be very low as a percentage of the rated capacity.) Finally, Section VI discusses the benefits of diverse locations in enhancing the load-carrying ability of tidal generation, and conclusions are given in Section VII.

## II. CAPACITY VALUE ANALYSIS

### A. Definition and Purpose of Capacity Value

#### 1) Definition:

The concept of capacity value quantifies the contribution of generating units or technologies to securing demand. The specific definition used here is Effective Load Carrying Capability (ELCC), the extra demand which an additional generator can support without increasing the value of a chosen risk index [6]. Alternative definitions include comparison with the load carrying capability of conventional plant [7], and definitions in terms of a given percentile of the distribution for available capacity from the new generation. We prefer ELCC, as it does not depend on the properties of a test unit (c.f. the 1st alternative), and is directly related to system risk (c.f. the 2nd).

#### 2) Purpose:

The importance of the concept of capacity value lies in the transparency of the results. A full risk calculation (e.g. that underlying the ELCC method presented next) provides the most comprehensive view of system risk within the scope of the calculation. However, such complex algorithms generally are not very transparent in demonstrating which factors drive the results which are obtained. This is why capacity value calculations are important; they provide a means of visualising the contribution of different generating units and technologies to supporting demand.

Unlike load factor over a period (which is defined as [mean output] / [rated capacity]), the 'capacity value' is not a quantity which can be calculated directly from observed data. Indeed, as there are a variety of possible definitions and calculation methods, there is not (even in principle) a single definitive value for the capacity value of a given generator. The capacity value should therefore be seen as an indicative quantity used or a visualisation tool, rather than something more precise.

### B. ELCC Calculation

#### 1) General Approach:

J. Radtke and S.J. Couch are with the School of Engineering, The University of Edinburgh, Mayfield Road, Edinburgh EH9 3JL, UK (Email: johannes.radtke@gmx.de, chris.dent@ed.ac.uk, Scott.Couch@ed.ac.uk).

C.J. Dent is with the School of Engineering and Computing Sciences, Durham University, South Road, Durham DH1 3LE, UK (Email: chris.dent@durham.ac.uk).

CJD was funded for this work through the EPSRC Supergen V, UK Energy Infrastructure (AMPerES) grant in collaboration with UK electricity network operators working under Ofgem's Innovation Funding Incentive scheme – full details on <http://www.supergen-amperes.org/>. SJC was funded for this work through the EPSRC Supergen Marine consortium.

The informal description of ELCC presented above is made more specific by the following two-point algorithm for calculating the ELCC of additional generation on a system:

- 1) Calculate the value  $I_0$  of the chosen risk index without the additional generation.
  - 2) Introduce the additional generation to the risk calculation. The risk index will then decrease if the demand level remains the same. The ELCC of the additional generation is the extra peak demand which returns the risk index's value to  $I_0$ .
- 2) *Choice of Risk Index:*

The aspect of risk considered in capacity value calculations is usually system adequacy, defined as the ability of the system to support demand in steady state (as opposed to system security, which is the ability to respond to sudden disturbances). The risk index used here is Loss Of Load Expectation (LOLE) [8]:

- The Loss Of Load Probability (LOLP) at any time is the probability that generation is insufficient to meet demand:

$$I_t^{\text{LOLP}} = p(X_t + R_t < D_t), \quad (1)$$

where  $X$  is the available conventional capacity,  $D$  the demand, and  $R$  the available renewable capacity (all are random variables in the most general formulation).

- The LOLE over a period is then the expected number of sub-periods (in this case half-hours) in which the available generation cannot support demand, or equivalently the sum over sub-periods of the LOLPs:

$$I^{\text{LOLE}} = \sum_t I_t^{\text{LOLP}}. \quad (2)$$

The historic demands might be scaled using a measure of underlying (weather corrected) peak demand level, so that the risk calculation is performed for a chosen future predicted demand level.

Risk indices which look at the volume of demand not supplied are also available; these might be regarded as giving a more detailed picture of risk, but in an application such as capacity values where only comparisons between different circumstances are required, this is likely to deliver very similar results to the computationally simpler LOLE index.

### 3) *Evaluating LOLE With Renewables:*

There are two common approaches to including renewables in an LOLE calculation, using either:

- a probabilistic model for the available renewable capacity, based on historic data [9], or
- the historic time series directly in the risk calculation, modelling renewable output as negative demand [10];  $n$  versions of a future study year could then be simulated using the renewable output and demand from  $n$  historic years.

The second (time series) approach is used here, as it naturally and straightforwardly captures the available statistical information on the relationship between resource availability and demand; despite the predictability of tidal heights, the long-term tidal resource is not necessarily the same across all times of day. The potential for a probabilistic representation of tidal

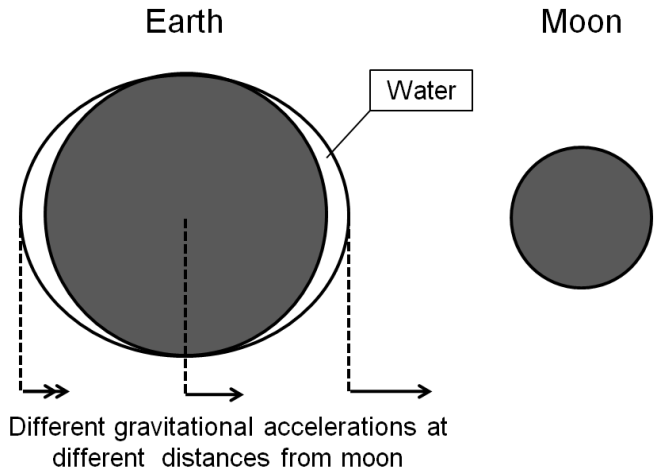


Fig. 1. Illustration of how the differential gravitational acceleration of the earth and seas causes lunar tides.

availability will be discussed in Section V. The next section will show how a realistic ‘hindcast’ time series for tidal output may be produced, as tidal cycles are completely predictable.

## III. MODELLING TIDAL BARRAGE GENERATION

### A. *Origin of Tides*

#### 1) *Equilibrium Theory of Tides:*

Oceanic tides on the earth are driven by the gravitational attraction of the moon and the sun, and specifically the differential acceleration of the oceans on the earth's surface, relative to that of the earth's centre of gravity. For simplicity, lunar tides will be described first; for more detail, see pp. 4150 of [11], [12].

The earth and the moon orbit about their mutual centre of gravity, with the required centripetal acceleration being driven by their mutual gravitational attraction. Because it is a rigid body, the gravitational acceleration of all solid parts of the earth must be the same as that of its centre of mass. However, as it is closer to the moon, the gravitational acceleration of water on the surface of the earth nearest to the moon is greater than that of the earth itself; as a result, this water follows a slightly smaller orbit than the part of the earth immediately underneath, and bulges outwards slightly from the earth's surface. Conversely, the water on the earth's surface which is furthest from the moon experiences a smaller acceleration than the part of the earth's surface immediately underneath. This effect is illustrated in Fig. 1.

2) *Multiple Tidal Cycles:* The previous paragraph describes the origin of the lunar tidal cycle. The sun generates a tidal component in the same way, the solar tides in isolation being about half the size of the lunar tides.

There are several different periodic cycles which affect the tidal ranges, the most important being the lunar tidal cycle (period 12.4 hours, the familiar approximately twice-daily cycle) and the solar tidal cycle (usually interpreted as variation in the difference in sea level between low and high tides, with a period of approximately 1 month). The tidal range is greatest when the lunar and solar high tides coincide (‘spring tides’),

and smallest when they are in anti-phase (‘neap tides’). The part of the lunar cycle where the sea level is rising is known as the flood tide, and the part where the sea level is falling is known as the ebb tide.

### 3) Local Geographical Effects:

The equilibrium theory described above explains the the existence of tides, including the temporal cycles in tidal behaviour; however, it cannot directly explain the local variations in amplitude caused by the shape of the seabed and coastlines. These modify the response of the oceanic waters to the gravitational tide generating forces [13]. In some parts of the world, coastal and seabed conditions result in extreme tidal current speeds, and also extreme tidal ranges (the height difference between high and low tides).

Either of these extreme effects can be used to generate electricity. This paper will confine itself to tidal barrage generation, which exploits the difference in height between high and low tides. A detailed description of tidal current generation, which exploits the velocity of tidal currents directly (typically using an ‘underwater wind turbine’-like device), may be found in [14]; an investigation of tidal current generation’s contribution to supporting demand may be found in [4].

### 4) Predictability:

Because tides are ultimately driven by the gravitational forces acting between bodies in periodic orbits, they are almost perfectly predictable over timescales of centuries (some small perturbations might be caused by local meteorological factors.) For this work, the Totaltide package [15], produced by the UK Hydrographic Office, has been used to generate tidal height data for the Severn Barrage site on a half-hourly time resolution; this matches the time resolution of the publicly-available Great Britain demand data [16].

## B. Tidal Barrage Generation

As described above, tidal barrage power plants exploit the difference in sea level between high and low tides to generate electrical energy [17] (see Fig. 2 for a map of the proposed Severn scheme, which illustrates the generic layout of barrage schemes.) The two most important examples of existing barrage schemes are on La Rance in France, and in the Bay of Fundy in Canada [18], [19].

For ebb generation, which is modelled here, water is allowed into the basin through sluices in the barrage during the flood tide; these are then closed at high tide. Generation would then occur on the ebb tide, once a sufficient head is available for the turbines to operate.

Other classes of tidal barrage schemes are available [19]–[21], using different combinations of generation on flood and ebb cycles, and pumping to increase the available head. However, ebb-only generation is typically found to maximise the value of a scheme’s energy production [22]; the typical U-shape of estuary cross-sections permits more water to flow through the turbines at the highest heads. Small barrage schemes, where the dam makes up all or most of the boundary of the tidal basin, are sometimes referred to as tidal lagoon schemes [23].

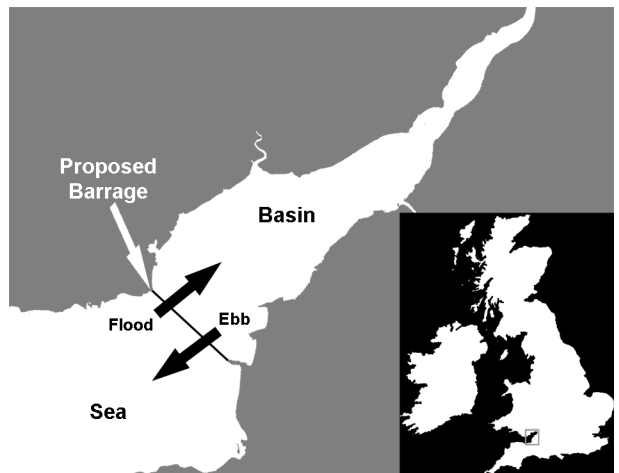


Fig. 2. Map showing the proposed 8 GW tidal barrage scheme on the Severn Estuary; water would enter the basin through sluices on the flood tide, and generation would occur on the ebb tide.

## C. The Severn Barrage Scheme

This paper discusses a barrage across the Severn Estuary from Cardiff to Weston Super-Mare [2], [24]; this is shown on the map in Fig. 2. The peak tidal range in the Severn Estuary is approximately 13m, one of the highest in the world.

The barrage as modelled is equipped with 216 kapeller turbines, as proposed in [2]. These are arranged in 9 groups of 24 turbines [25]. For simplicity, it is assumed here that turbines operate either at zero or the greatest possible output given the available head, and that only whole turbine groups (as opposed to individual turbines) may be switched on or off; this assumption is not expected to affect the conclusions significantly. It is further assumed that any any time 95% of turbines are mechanically available.

The turbine efficiency is taken as 90% for heads above 4m, and varies linearly from 70% to 90% for heads between 1.5m and 4m; for heads below 1.5m, generation stops. The power output from a single turbine varies linearly from 0 MW at 1.5m head to 40 MW (rated capacity) at 4m head; for any head above 4m, a constant 40 MW is available (see Fig. 3). The fixed and variable parts of each turbine generator’s electrical losses are respectively 2.5%, and varying quadratically between 0 and 2.2%, of the turbine’s maximum output.

The available output and corresponding discharge rate for a single turbine are shown in Fig. 3; the output is as defined above, and the corresponding discharge rate is calculated as described in Section III-D. These curves are similar to those for real turbines described in [19], [23], [26].

## D. Modelling of Barrage Output

The average power output per turbine from an ebb-only tidal barrage during a time period  $n$  may be calculated as [21]:

$$P_n^{\text{turb}} = \frac{\rho g h_n \eta Q_n}{T_n}, \quad (3)$$

where  $P_n^{\text{turb}}$  is the output per turbine,  $\rho$  is the density of sea water (taken as  $1030 \text{ kgm}^{-3}$ ),  $g$  the acceleration due to gravity

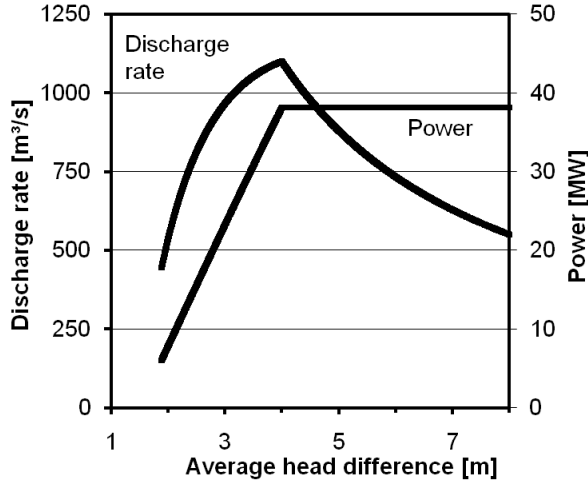


Fig. 3. Turbine performance curves, giving discharge rate and output power per turbine as a function of head.

(taken as  $9.81 \text{ ms}^{-2}$ ),  $h_n$  the average head difference across the barrage in period  $n$ ,  $\eta$  the turbine efficiency,  $Q_n$  the water volume per turbine discharged in  $\text{m}^3$ , and  $T_n$  the length of period  $n$ . The assumptions required are that the water surfaces upstream and downstream of the barrage are both horizontal, and that the upstream and downstream water surface areas remain constant. The derivation is based on the gravitational potential energy lost by the water passing through the turbines.

The operational choice to be made for period  $n$  is, in the simplified model used here, the number of turbine groups to run. The discharge rate in period  $n$ , is then a function (of as yet unknown value) of the mean head  $h_n$ ; the efficiency and output per turbine are also functions of  $h_n$ , whose values are as defined in Section III-C. It is therefore necessary to solve (equivalently) for the discharge volume or average head in period  $n$ , which may be achieved by eliminating  $h_n$  from (3).

The level of the tidal basin at the end of period  $n$ ,  $h_n^B$ , is

$$h_n^B = h_{n-1}^B - \frac{Q_n N_n}{A}, \quad (4)$$

where  $T_n$  is the length of period  $n$ ,  $N_n$  is the number of turbines running, and  $A$  is the surface area of the water behind the barrage. The average head in period  $n$  is

$$h_n = \frac{h_n^B + h_{n-1}^B - h_n^S - h_{n-1}^S}{2}, \quad (5)$$

where  $h_n^S$  is the sea level at the end of period  $n$ . Eliminating  $h_n^B$  from (5) gives

$$2h_n = 2h_{n-1}^B - (h_n^S + h_{n-1}^S) - \frac{Q_n(h_n)N_n}{A}. \quad (6)$$

Finally, substituting this expression for  $h_n$  in (3),

$$Q_n = \frac{P_n^{\text{turb}}(h_n)T_n}{\rho g \eta(h_n) \left( h_{n-1}^B - \frac{h_n^S + h_{n-1}^S}{2} - \frac{Q_n N_n}{2A} \right)} \quad (7)$$

This may be solved for  $Q_n$  by formula iteration. After each iteration, the value of  $h_n$  is updated using (6), and using this the values for  $P_n^{\text{turb}}(h_n)$  and  $\eta(h_n)$  are in turn updated. The discharge rate in Fig. 3 is derived using this method.

## IV. SEVERN BARRAGE CAPACITY VALUE: RESULTS

### A. Description of Risk Calculation

In this section, results for the effective load-carrying capability of the Severn Barrage project are presented; the ELCC calculation is as described in Section II. The input data to the risk calculation described above is as follows:

- *Demand data.* Half-hourly time series Great Britain demand data from the winters of 2005 to 2009 is used [16].
- *Choice of peak demand level.* Each winter's demands are scaled to give an ACS peak demand level (Average Cold Spell – the measure of underlying weather-corrected demand level used in GB) of 61 GW.
- *Conventional generation.* The distribution for available conventional generation is as described in [27]; it is based on unit capability data supplied by the system operator, and generated from a capacity outage table calculation [8]. The calculated mean and standard deviation of the available conventional capacity are 64.88 and 1.92 GW.

### B. Capacity Value Results

#### 1) Operational Modes Considered:

Three operational modes will be considered here; in each case the following decisions must be made for each tidal cycle:

- How many turbines to run.
- How long after high tide to start operation.

The three modes are:

- *'Constant'*. Same number of turbine groups for all tidal cycles. Start times chosen to maximise energy output.
- *'Variable'*. The number of turbine groups operating in a tidal cycle is chosen according to the tidal range  $h^R$  in that cycle. A minimum of one turbine group is run. If  $h^R$  exceeds 5 m, then a second turbine is run. For each further 0.6 m of tidal range, another turbine is added. The start time for each cycle chosen to maximise energy output.
- *'MinRisk'*. As with *Constant*, the same number of turbine groups is run in all tidal cycles. However, the start time for each tidal cycle chosen to maximise the sum over half hours in the cycle of ( $[\text{Power output}] \times [\text{LOLP without barrage}]$ ). This mode ensures that the barrage makes the greatest possible capacity available at times of highest demand. Clearly this policy would not be financially optimal for the barrage if followed over all cycles. However, a capacity value calculation is about what the generator *can* do when needed, not what it *will* do when system margin is not tight.

This range of modes does not cover all possible operational modes, but is sufficient to illustrate the important interplay between energy maximisation and system risk minimisation.

#### 2) Results: Energy Maximisation:

Total energy output over the four winters, and ELCC, are shown in Table I for mode *Constant* with 7, 8 and 9 turbine groups operating, and also for mode *Variable* with a maximum of 7, 8 or 9 groups operating. Several trends may be observed:

- As the number of turbines run goes down (either moving from *Constant* to *Variable*, or reducing the maximum

TABLE I  
ENERGY OUTPUT AND CAPACITY VALUE RESULTS FOR OPERATIONAL  
MODES *Constant* AND *Variable*.

	Mode	Energy [TWh]	ELCC [MW]	ELCC [%]
9 turbine groups	<i>Constant</i>	34.54	286	3.3%
	<i>Variable</i>	31.51	496	5.7%
	Change	-8.8%	+73%	
8 turbine groups	<i>Constant</i>	33.05	311	4.0%
	<i>Variable</i>	30.66	499	6.5%
	Change	-7.2%	+60%	
7 turbine groups	<i>Constant</i>	31.40	331	4.9%
	<i>Variable</i>	29.47	510	7.6%
	Change	-6.1%	+54%	

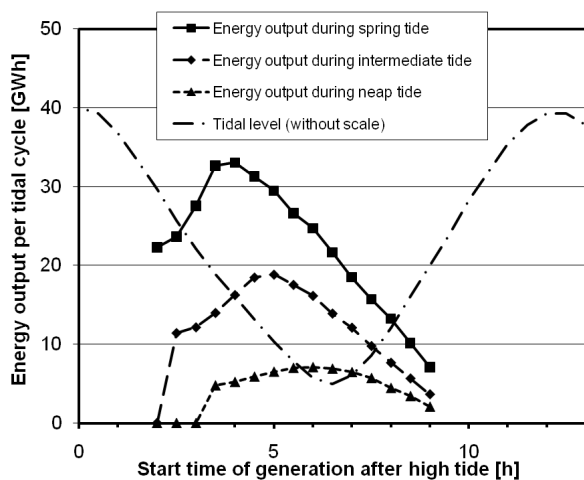


Fig. 4. Energy output versus start time, for spring, neap and intermediate tides.

number), the energy output decreases. This is because, in raw energy terms, it is optimal to generate as hard as possible when the available power is at its greatest.

- As the number of turbine groups run decreases, the ELCC increases. This is because decreasing the number of groups increases the number of hours in which power is generated, and hence increases the effective availability probability of the barrage.
- The ELCC is very low as a percentage of rated capacity.

The last two points will be discussed further in Section V.

The effect on energy output of shifting the generation start time are further illustrated in Fig. 4, which plots energy output in the tidal cycle against start time of generation, assuming that all nine turbine groups are run at maximum output once generation has begun. For maximising energy, the optimal start time is about 4 hours after high tide for a spring tide, with the delay increasing to six hours for a neap tide.

### 3) Results: Risk Reduction:

The MinRisk mode described in Section IV-B1 seeks to maximise over the course of a cycle the time integral of ([LOLP without barrage]  $\times$  [power output]). On the planning timescale considered here, this means of focusing on the hours of highest demand will allow exploration of the highest long-term capacity value achievable. On an operational timescale,

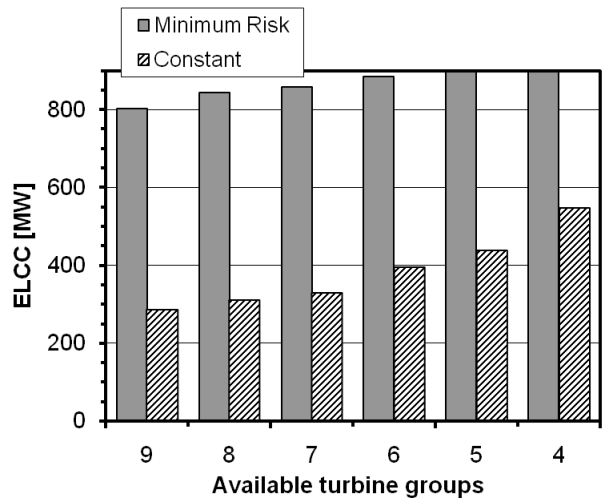


Fig. 5. Comparison of capacity values between *MinRisk* and *Constant* modes.

it would be possible to focus directly on hours when margin is known to be tight (on a 12-hour lead time there will be a fairly accurate assessment of the availability of other generators). If the barrage's goal is to maximise income, then electricity price spikes will provide the necessary financial incentive to maximise output at times when system margin is tight.

It should be emphasised once more that, while the energy output might be low on tidal cycles where the barrage's output is modified to support peak demand when margin is tight, this will not impact significantly on total energy output over the course of a year; when the system margin is comfortable, which it is in most tidal cycles, income will be maximised by near-maximising energy output.

Results from this risk-minimising mode are compared with the energy-maximising mode considered earlier in Fig. 5. As before, the capacity value increases as the number of turbines used decreases (and hence the barrage operates for more of the time). As would be expected, the Minrisk mode results in a higher MW capacity value, although the capacity value is still small as a percentage of the barrage's total rated capacity.

## V. TIDAL BARRAGE CAPACITY VALUE: PROBABILISTIC MODEL

### A. Description

These surprisingly low ECCC values may be explained using a simple probabilistic model, which assumes:

- Fixed demand  $d$  of 60 GW.
- Normal distribution for available conventional capacity  $X$ , with mean 64.88 GW and SD 1.92 GW.
- Barrage modelled as a single two-state conventional unit, with available capacity  $c$  available with probability  $a$  at peak, and zero capacity available with probability  $1 - a$ .

The ELCC  $\delta d$  is then given by:

$$F_X(d) = aF_X(d + \delta d - c) + (1 - a)F_X(d + \delta d), \quad (8)$$

where  $F_X(d) = p(X \leq d)$  is the LOLP at demand  $d$ .

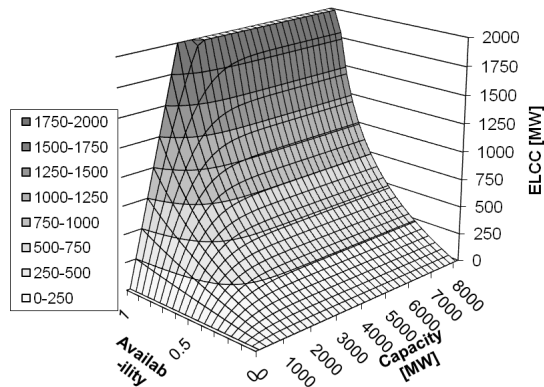


Fig. 6. Dependence of ELCC of two-state tidal barrage on capacity and availability.

### B. Results and Discussion

The dependence of the ELCC on the capacity  $c$  and availability probability  $a$  in the simple barrage model are shown in Fig. 6. As expected, for any installed capacity the ELCC increases as the availability probability increases. The ELCC increases with installed capacity up to capacities of about 2 GW, but is then almost constant as the capacity increases further. This is because, for large capacities, when the barrage is available the half-hourly LOLP risk is reduced to almost zero; almost the same effect occurs independently of the precise installed capacity.

Because there is a very large probability of zero available capacity (for an ebb-only scheme the barrage must be available to generate for less than half the time), the resulting ELCC is very small as a percentage of rated capacity. As the ELCC does not depend strongly on the installed capacity for large barrages, it is more appropriate to express the value in MW, rather than as a percentage of installed capacity.

## VI. DISCUSSION

### A. Benefits of Diversity

This work has considered the ELCC of a single tidal scheme, added to an otherwise all-conventional system, in isolation. As mentioned in Section III, the tides are completely predictable many years ahead. As a consequence, if the tidal cycles at two different sites are out of phase with each other, this will enhance the ELCC of the combined tidal generation fleet, as the probability of neither being available is much reduced.

Fig. 7 illustrates this for possible British sites at the Severn and Mersey Estuaries, and the Solway Firth. As the Solway and Mersey tides are almost in antiphase with the Severn, their combined available output is guaranteed to be non-zero for a much higher proportion of the time than that of any individual scheme. This would however not connect the load-carrying ability of the Severn scheme directly to its related capacity, as the potential rated capacity of this scheme is considerably greater than that of all other potential GB tidal schemes combined; the same picture of a very large barrage

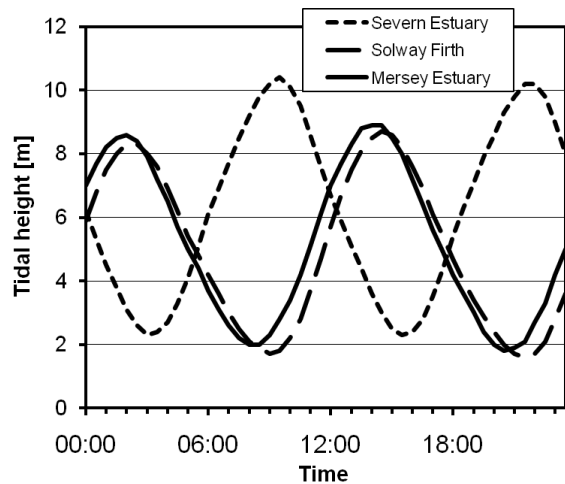


Fig. 7. Tides at Severn, Mersey and Solway estuary on 1 January 2009.

reducing risk to near-zero when available, and this effect being independent of its precise capacity, would still apply.

### B. Probabilistic Representation of Tidal Availability

This paper has presented a time-series hindcast based ELCC analysis for tidal barrage generation. This use of historic time series is widely seen as the preferred approach for calculating the ELCC of wind generation, as incorporating the relationship between wind availability and demand correctly within a probabilistic wind model is not straightforward [28]; the time-series approach automatically takes into account the available statistical information regarding this relationship.

As tidal cycles are completely predictable over many years, deriving a probability distribution for the tide height at any site at time of peak demand is quite straightforward (this probability distribution is not necessarily the same at all times of day.) However, as illustrated above, the available capacity from tidal barrages at a given time is not a function of the physical resource parameters at that time alone; a further input required for a capacity-value calculation is the operational policy which maximises availability at time of peak demand. Deriving a probability distribution for available tidal capacity at time of peak demand is therefore not straightforward.

However, as an almost unlimited amount of tidal data is available, such a probabilistic representation of tidal availability might provide a better estimate of the adequacy risk than the time series approach; it takes into account all possible tidal scenarios in the small number of half hours of high demand which dominate the risk, as opposed to considering just the scenarios which were actually realised over the period considered.

## VII. CONCLUSIONS

This paper has presented the first detailed capacity value calculation for large scale tidal barrage generation. The key finding is that the Effective Load Carrying Capability is very low as a percentage of installed capacity (less than 10% for the

example presented here). This is due to the high probability of having zero available output at time of peak demand, due to the possibility of peak demand occurring on the wrong part of the diurnal tidal cycle.

Tidal barrage might therefore be regarded as a truly intermittent form of generation (there is a debate over whether wind should be called intermittent or variable, as the probability of it having precisely zero available capacity is small.)

It is thus more natural to express the ELCC as a MW value, rather than a percentage of rated capacity. When available, a very large barrage reduces the generation adequacy risk to near zero, an effect which does not depend on its precise capacity; as a result, for large barrages the ELCC is also independent of the installed capacity of the barrage.

## REFERENCES

- [1] G. Boyle, Ed., *Renewable Energy – Power for a Sustainable Future*. OUP, 2004.
- [2] “Turning the Tide, Tidal Power in the UK,” Sustainable Development Commission, Tech. Rep., Oct. 2007.
- [3] C. Ensslin, M. Milligan, H. Holttinen, M. O’Malley, and A. Keane, “Current methods to calculate capacity credit of wind power,” in *IEEE PES General Meeting*, July 2008.
- [4] A. G. Bryans, B. Fox, P. A. Crossley, and M. O’Malley, “Impact of tidal generation on power system operation in Ireland,” *IEEE Trans. Power Syst.*, vol. 20, no. 4, pp. 2034–2040, Nov. 2005.
- [5] “Implementation of EU 2020 Renewable Target in the UK Electricity Sector: Renewable Support Schemes,” Trilemma UK, University of Cambridge, and Redpoint, Tech. Rep., 2008.
- [6] L. L. Garver, “Effective load carrying capability of generating units,” *IEEE Trans. Power Apparatus and Systems*, vol. 85, no. 8, August 1966.
- [7] M. Milligan and K. Porter, “Determining the capacity value of wind: An updated survey of methods and implementation,” in *WindPower 2008*, Houston, Texas, June 2008.
- [8] R. Billinton and R. N. Allan, *Reliability evaluation of power systems, 2nd edition*. Plenum, 1994.
- [9] C. D’Annunzio and S. Santoso, “Noniterative method to approximate the effective load carrying capability of a wind plant,” *IEEE Trans. Energy Conv.*, vol. 23, no. 2, pp. 544–550, June 2008.
- [10] M. Amelin, “Comparison of capacity credit calculation methods for conventional power plants and wind power,” *IEEE Trans. Power Syst.*, vol. 24, no. 2, May 2009.
- [11] E. Brown, A. Colling, D. Park, J. Phillips, and D. Rothery, *Waves, Tides and Shallow-Water Processes*. Butterworth-Heinemann, The Open University, Oxford.
- [12] C. Johnson, “Mathematical explanation of tides,” <http://mb-soft.com/public/tides.html>, accessed 23 Aug. 2009.
- [13] I. G. Bryden, S. J. Couch, A. Owen, and G. Melville, “Tidal Current Resource Assessment,” *Proc. IMechE Part A: J. Power and Energy*, vol. 221, pp. 125–135, 2007.
- [14] I. G. Bryden, T. Grinstead, and G. T. Melville, “Assessing the potential of a simple tidal channel to deliver useful energy,” *Applied Ocean Research*, vol. 26, no. 5, pp. 198–204, July 2004.
- [15] “Total Tide version 1.4.0.2,” United Kingdom Hydrographic Office, Tech. Rep., 2004, see <http://www.ukho.gov.uk/ProductsandServices/DigitalPublications/Pages/ATT.aspx>.
- [16] “National Grid: Demand Data,” available at <http://www.nationalgrid.com/uk/Electricity/Data/Demand+Data/>.
- [17] R. H. Charlier and C. W. Finkl, *Ocean Energy – Tide and Tidal Power*. Springer, 2009.
- [18] R. Charlier, “Forty candles for the Rance river tbpp tides provide renewable and sustainable power generation,” *Renewable and Sustainable Energy Reviews*, vol. 11, no. 9, pp. 2032–2057, Dec. 2007.
- [19] A. C. Baker, *Tidal Power*. Peter Peregrinus, 1991.
- [20] L. B. Bernshtein, *Tidal Energy for Electric Power Plants*, 1965.
- [21] D. Prandle, “Simple theory for designing electric power schemes,” *Advances in Water Resources*, vol. 7, no. 1, pp. 21–27, March 1984.
- [22] “Tidal Power,” IET, available at [www.theiet.org/factfiles](http://www.theiet.org/factfiles).
- [23] “Tidal Lagoon Power Generation Scheme in Swansea Bay,” Department of Trade and Industry and the Welsh Development Agency, Tech. Rep., April 2006, uRN: 06/1051.
- [24] “Severn Barrage Project General Report,” Severn Tidal Power Group and Department of Energy, Tech. Rep., 1989, energy Paper 57, HMSO.
- [25] “Severn Barrage Project Detailed Report, Volume II: Electrical and Mechanical Engineering,” Severn Tidal Power Group and Department of Energy, Tech. Rep., 1989, eTSU TID 4060-P2.
- [26] R. Clare, *Tidal power: trends and developments*, 1992.
- [27] P.E. Olmos Aguirre, C. J. Dent, and J. W. Bialek, “Realistic calculation of wind generation capacity credits,” in *Cigre/IEEE PES Symposium on Integration of Wide-Scale Renewable Resources*, July 2009.
- [28] C. J. Dent, A. Keane, and J. W. Bialek, “Simplified Methods for Renewable Generation Capacity Credit Calculation: A Critical Review,” in *IEEE PES General Meeting*, 2010.